Viscoelastic Response of a Complex Fluid at Intermediate Distances

Adar Sonn-Segev,[1] Anne Bernheim-Groswasser,[2] Haim Diamant,[1] and Yael Roichman[1,*]
[1]Raymond and Beverly Sackler School of Chemistry, Tel Aviv University, Tel Aviv 6997801, Israel
[2]Department of Chemical Engineering, Ilse Kats Institute for Nanoscale Science and Technology, Ben Gurion University of the Negev, Beer-Sheva 84105, Israel

(Received 16 July 2013; revised manuscript received 3 October 2013; published 25 February 2014)

The viscoelastic response of complex fluids is length- and time-scale dependent, encoding information on intrinsic dynamic correlations and mesoscopic structure. We study the length scale above which bulk viscoelasticity sets in, and the material response that precedes it at shorter distances. We show that the crossover between these two regimes may appear at a surprisingly large distance. We generalize the framework of microrheology to include both regimes and apply it to F-actin networks, thereby extracting their dynamic correlation length from their bulk and local viscoelastic properties.

DOI: 10.1103/PhysRevLett.112.088301 PACS numbers: 47.57.Qk, 87.16.dm, 87.16.dj, 87.16.Ln

Most fluids in nature and industry are complex, or structured [1], in the sense that they include mesoscopic elements in between the molecular and macroscopic scales. For example, in suspensions, micron-scale solid particles are dispersed in a molecular fluid, and in polymer gels the polymer chains form a network embedded within a molecular solvent. Consequently, the response of complex fluids to stress is characterized by intermediate length and time scales.

The bulk viscoelastic response of such materials is commonly measured using macrorheology [2]. Similar information, for a wider frequency range and smaller material quantity, can be extracted from microrheology by following the motions of embedded tracer particles [3–8]. In one-point (1P) microrheology [3–5] the thermal fluctuations of a single particle are used to infer the viscoelastic properties of the medium via a generalized Stokes-Einstein relation (GSER). It has been found that this measurement is affected by the local environment of the tracer particle [9,10], and thus, may fail to reproduce the material's bulk response. Two-point (2P) microrheology [6] overcomes this obstacle by tracking the correlated motions of particle pairs as a function of their separation. 2P measurements have focused on asymptotically large separations, where the pair correlation has a universal form due to momentum conservation.

The current Letter addresses two questions: (i) Beyond what length scale does the bulk viscoelastic behavior emerge? (ii) What is the material response at smaller length scales? We find that the leading correction to the asymptotic behavior at large distances, referred to, hereafter, as the subdominant response, may be unexpectedly large, causing the bulk response to set in at surprisingly large distances. The physical origin of the subdominant response, which is unique to complex fluids, is different from that of the asymptotic one. It is related as well to a conservation law (of fluid mass rather than momentum), resulting in a generic system-independent form. The study of this distinctive regime leads to a more complete description of the complex-fluid response.

We first derive the generic form of the subdominant response and, subsequently, confirm the general predictions in a specific theoretical example, the two-fluid model of polymer gels [8,11,12]. Extending the framework of microrheology to include the subdominant term, we validate its significant effect in a model experimental system, entangled F-actin networks of various concentrations.

We set the stage by recalling the classical Stokes problem of a rigid sphere of radius a, driven by a steady force $\mathbf{F}$ through an incompressible fluid of viscosity η [13]. The fluid velocity at position $\mathbf{r}$ away from the sphere's center is given by $\mathbf{v}(\mathbf{r}) = \mathbf{v}_1 + \mathbf{v}_2$, with $v_{1\alpha} = (8\pi\eta r)^{-1}(\delta_{\alpha\beta} + \hat{\mathbf{r}}_\alpha\hat{\mathbf{r}}_\beta)F_\beta$ and $v_{2\alpha} = a^2(24\pi\eta r^3)^{-1}(\delta_{\alpha\beta} - 3\hat{\mathbf{r}}_\alpha\hat{\mathbf{r}}_\beta)F_\beta$, where Greek indices denote the coordinates (x, y, z), and repeated indices are summed over. The dominant term at large distances, $\mathbf{v}_1$, is the flow due to a force monopole $\mathbf{F}$. Its r^{-1} decay is dictated by momentum conservation, ensuring that the integrated momentum flux (proportional to $\nabla\mathbf{v}_1 \sim r^{-2}$) through any closed surface around the sphere remain fixed. This dominant response can be decomposed into longitudinal and transverse components (force and velocity parallel and perpendicular to $\mathbf{r}$, respectively), $v_{1\parallel} = (4\pi\eta r)^{-1}F_\parallel$, $v_{1\perp} = (8\pi\eta r)^{-1}F_\perp$, both of which are positive. Turning to the subdominant $\mathbf{v}_2$, we point out the largely overlooked fact that it is actually made of two contributions, having the same spatial form but opposite signs and different physical origins, $\mathbf{v}_2 = \mathbf{v}_{2f} + \mathbf{v}_{2m}$. The first, $\mathbf{v}_{2f} = 3\mathbf{v}_2$, is the flow due to a force quadrupole $Q_{\gamma\alpha\beta} = \frac{1}{2}a^2\delta_{\gamma\alpha}F_\beta$. We focus our attention on the opposite contribution, $\mathbf{v}_{2m} = -2\mathbf{v}_2$. It is the flow due to a mass dipole $\mathbf{m} = -[a^2/(3\eta)]\mathbf{F} = -2\pi a^3\mathbf{U}$, created opposite to the direction of the sphere's displacement, where $\mathbf{U} = (6\pi\eta a)^{-1}\mathbf{F}$ is the sphere's velocity. The net subdominant term introduces a negative correction to the

longitudinal response, $v_{2\parallel} = -a^2(12\pi\eta r^3)^{-1}F_\parallel$, and a positive correction to the transverse one, $v_{2\perp} = a^2(24\pi\eta r^3)^{-1}F_\perp$. Since the simple fluid has no intrinsic length scale, these corrections vanish as $a \to 0$.

Now, contrast the above with the case of an isotropic viscoelastic medium [14], having a frequency-dependent complex shear modulus $G(\omega) = G'(\omega) + iG''(\omega)$ [i.e., bulk shear viscosity $\eta_b(\omega) = G(\omega)/(-i\omega)$]. Dynamic correlations in the medium (as measured, e.g., by dynamic scattering) decay with a characteristic correlation length ξ_d, which in polymer solutions is believed to coincide with the static mesh size ξ_s [11]. Consider a sphere of radius a, driven through the medium by an oscillatory force $\mathbf{F}e^{-i\omega t}$. At sufficiently large distances the medium velocity must be dominated by the monopolar $v_{1\alpha} = (8\pi\eta_b r)^{-1}(\delta_{\alpha\beta} + \hat{\mathbf{r}}_\alpha\hat{\mathbf{r}}_\beta)F_\beta$, for the same momentum-conservation reasons given above. This is the basis of present 2P microrheology [6–8]. The two subdominant r^{-3} contributions, however, become separated. Consider first the limit $a/\xi_d \to 0$, for which the separation is largest. (Because of the intrinsic length scale ξ_d, v_2 does not vanish in this case.) The force quadrupole, $Q \sim \xi_d^2 F$, creates a flow $v_{2f} \sim \xi_d^2(\eta_b r^3)^{-1}F$, dependent (like the monopolar v_1) on bulk viscosity. By contrast, the mass dipole in this limit arises from fluid displacement at scales smaller than ξ_d, where the relevant viscosity is the solvent's, η; hence, $m \sim -(\xi_d^2/\eta)F$, creating a flow $v_{2m} \sim -\xi_d^2(\eta r^3)^{-1}F$. Thus, v_{2m} is enhanced relative to v_{2f} by a factor of η_b/η, which is typically very large. In such a case of a large contrast between local and bulk response, the mass-dipole term takes over the subdominant response and changes its sign, $v_{2\alpha} \simeq v_{2m,\alpha} \sim -\xi_d^2(\eta r^3)^{-1}(\delta_{\alpha\beta} - 3\hat{\mathbf{r}}_\alpha\hat{\mathbf{r}}_\beta)F_\beta$. This has two distinctive consequences: (a) The corrections to the longitudinal and transverse responses flip signs, $v_{2\parallel} = \xi_d^2(\eta r^3)^{-1}F_\parallel$, $v_{2\perp} \sim -\xi_d^2(\eta r^3)^{-1}F_\perp$. (b) The crossover to the asymptotic r^{-1} term is pushed further to a distance $r_c \sim (\eta_b/\eta)^{1/2}\xi_d \gg \xi_d$. In the opposite limit of an arbitrarily large sphere, $a/\xi_d \to \infty$, only bulk properties matter, and we have $Q \sim a^2 F$, $m \sim -(a^2/\eta_b)F$, making v_{2f} and v_{2m} comparable again. To interpolate between the two limits, we define a local viscosity at the scale of the probe, $\eta_\ell \equiv F/(6\pi a U)$, as determined from the sphere's velocity [15]. Additionally, dimensionless scale functions may be introduced, satisfying $Q = a^2 f(\xi_d/a)F$ and $m = -(a^2/\eta_\ell)g(\xi_d/a)F$, such that both $f(x)$ and $g(x)$ interpolate between values ~ 1 for $x \ll 1$ and $\sim x^2$ for $x \gg 1$.

We demonstrate the validity of these predictions in the two-fluid model of a dilute polymer gel [8,11,12]. In this model, an incompressible viscous fluid with velocity field $\mathbf{v}(\mathbf{r}, t)$, pressure field $p(\mathbf{r}, t)$, and viscosity η, is coupled to a dilute elastic (or viscoelastic) network with displacement field $\mathbf{u}(\mathbf{r}, t)$ and Lamé coefficients μ and λ via a mutual friction coefficient Γ [16]. For a point force acting on the fluid component, one obtains for the fluid-velocity response in Fourier space $[(\mathbf{r}, t) \to (\mathbf{q}, \omega)]$ [8]

$$v_\alpha(\mathbf{q}, \omega) = \frac{1 + (\eta_b/\eta)\xi_d^2 q^2}{\eta_b q^2(1 + \xi_d^2 q^2)}(\delta_{\alpha\beta} - \hat{\mathbf{q}}_\alpha\hat{\mathbf{q}}_\beta)F_\beta, \quad (1)$$

with $\eta_b = \eta - \mu/(i\omega)$ and $\xi_d^2 = \eta\mu/[\Gamma(\mu - i\omega\eta)]$. Inverting back from $\mathbf{q}$ to $\mathbf{r}$ while assuming $\eta_b \gg \eta$, we get at large distances the two predicted terms, $\mathbf{v} \simeq \mathbf{v}_1 + \mathbf{v}_2$, where

$$v_{1\alpha} = \frac{\delta_{\alpha\beta} + \hat{\mathbf{r}}_\alpha\hat{\mathbf{r}}_\beta}{8\pi\eta_b r}F_\beta, \qquad v_{2\alpha} = -\frac{\xi_d^2(\delta_{\alpha\beta} - 3\hat{\mathbf{r}}_\alpha\hat{\mathbf{r}}_\beta)}{4\pi\eta r^3}F_\beta. \quad (2)$$

These results are for the limit $a/\xi_d \to 0$, where $\eta_\ell \to \eta$. We have calculated also the fluid-velocity response of this model to a forced rigid sphere of finite radius a. The ξ_d^2 coefficient in Eq. (2) is then modified to $a^2 g(\xi_d/a)$ with $g(x)$ given below [17]. The dominant response becomes equal to the subdominant one at the distance

$$r_c = a[2(\eta_b/\eta_\ell)g(\xi_d/a)]^{1/2}, \qquad g(x) = x^2 + x + 1/3. \quad (3)$$

These expressions were obtained assuming $\eta_b/\eta_\ell \gg 1$ and an incompressible network ($\lambda \to \infty$ or Poisson ratio $\sigma = 1/2$). A large η_b/η_ℓ ratio is expected, e.g., for small probes in stiff polymer networks [18]. Effects of compressibility [19] are found not to change Eq. (3) appreciably for σ as low as 0.4 [17].

Let us summarize the three main characteristics of the subdominant response, expected in a complex fluid with a large η_b/η_ℓ contrast: (a) a positive r^{-3} decay of the longitudinal response; (b) a negative transverse response; (c) a crossover to the asymptotic response at a distance much larger than the correlation length [20].

We use thermally equilibrated, homogeneous samples of entangled F-actin networks, whose rheology has been thoroughly characterized in recent years [6,21–24]. It is well established that 1P microrheology underestimates the bulk viscoelastic moduli of these networks, whereas a more accurate measurement is obtained by 2P microrheology [6,22–24]. The large contrast between the bulk and local moduli makes these networks a good model system for checking the aforementioned predictions. F-actin networks have the additional benefit of an easy control over the network's mesh size, $\xi_s = 0.3/\sqrt{c_A}$, determined by the monomer concentration c_A (c_A in mg/ml and ξ_s in μm) [25].

Entangled F-actin networks were polymerized from purified monomer G-actin in the presence of passivated polystyrene colloidal particles of radii $a = 0.245$ and 0.55 μm (Invitrogen) [26]. We set the average filament length to be ≈ 13 μm by addition of capping protein. The actin concentrations were $c_A = 0.46$–2 mg/ml, corresponding to $\xi_s = 0.44$–0.21 μm, respectively. Immediately after polymerization the sample was loaded into a glass cell, previously coated with methoxy-terminated polyethylene glycol to prevent binding of the network to the glass [26]. After equilibration for 30 min at room temperature, samples were fluorescently imaged at $\lambda = 605$ nm. Tracer particle

motion from approximately 8×10^5 frames per sample was recorded at a frame rate of 70 Hz and tracked with accuracy of at least 13 nm [27].

We start by characterizing the viscoelastic properties of the F-actin networks using conventional 1P and 2P microrheology. In 1P microrheology, one measures the ensemble-averaged mean-squared displacement (MSD) of individual tracer particles along any axis x as a function of lag time τ, $\mathrm{MSD}^{1P}(\tau) \equiv \langle \Delta x^2(\tau) \rangle$, and extracts from it the viscoelastic moduli, $G'(\omega)$ and $G''(\omega)$, using the GSER [3,7,28]. In 2P microrheology, one measures the ensemble-averaged longitudinal (parallel to $\mathbf{r}$) and transverse (perpendicular to $\mathbf{r}$) displacement correlations of particle pairs as functions of interparticle distance r and lag time τ, $D_\parallel(r,\tau)$, $D_\perp(r,\tau)$ [6]. At sufficiently large distances, both correlations decay as r^{-1}, $D_\parallel \simeq A(\tau)/r$ and $D_\perp \simeq A(\tau)/(2r)$. The common practice is to use this asymptote to define a "two-point mean-squared displacement," $\mathrm{MSD}^{2P}(\tau) \equiv 2A(\tau)/(3a)$ [29], and extract from it the viscoelastic moduli using again the GSER [6]. Figures 1(a) and 1(b) show the 1P and 2P MSD's measured in an actin network and the moduli extracted from them. The measurements demonstrate the much softer local environment probed by the 1P technique, compared to the bulk response probed by the 2P one. These results are in quantitative agreement with previous studies on F-actin networks [6,22,23].

A closer look at the 2P longitudinal correlation reveals a positive r^{-3} decay preceding the asymptotic r^{-1} one [Fig. 1(c)]. The crossover between the two regimes appears

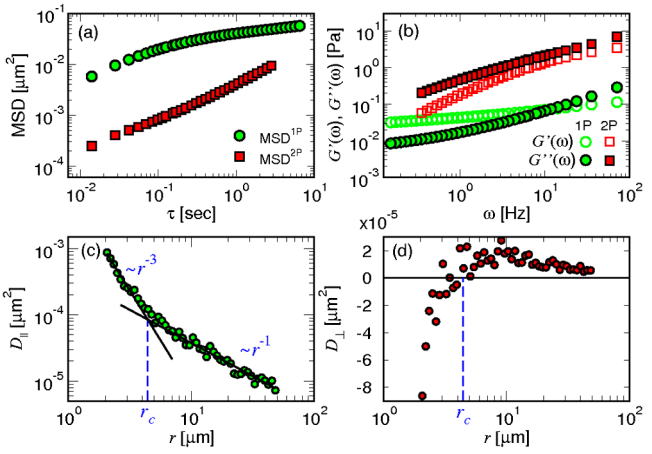

FIG. 1 (color online). Microrheology of entangled F-actin networks. (a) MSD^{1P} (green) and MSD^{2P} (red) as a function of lag time, for $\xi_s = 0.3$ μm and $a = 0.245$ μm. (b) The storage modulus $G'(\omega)$ (open symbols) and loss modulus $G''(\omega)$ (filled symbols), extracted from the MSD^{1P} (green) and MSD^{2P} (red) curves of panel (a). (c) Longitudinal and (d) transverse displacement correlations as a function of particle separation at lag time $\tau = 0.014$ s for $\xi_s = 0.44$ μm and $a = 0.55$ μm. The crossover distance r_c (blue dashed line) is defined at the intersection of the fitted dominant (r^{-1}) and subdominant (r^{-3}) power-law decays of $D_\parallel$.

at a distance $r_c = 4.4$ μm, an order of magnitude larger than the network mesh size ξ_s. For $r < r_c$ the transverse correlation is found to be negative [Fig. 1(d)]. Thus, the three qualitative features mentioned above for the intermediate response are verified.

Now, we extend the formalism of microrheology to include the response at intermediate distances. This has two goals: (a) to validate in more detail the theoretical predictions; (b) to provide a quantitative analysis to be used in future studies of other complex fluids. We focus on the longitudinal displacement correlation, $D_\parallel(r,\tau)$, which is stronger than the transverse one, and apply it in the time (rather than frequency) domain to minimize data manipulation.

The correlation can be well fitted over both large and intermediate distances by

$$D_\parallel(r,\tau) = A(\tau)/r + B(\tau)/r^3. \tag{4}$$

There are three directly measured quantities: $\mathrm{MSD}^{1P}(\tau)$; $A(\tau)$ or, equivalently, $\mathrm{MSD}^{2P}(\tau)$; and $B(\tau)$. We need to relate them to the frequency-dependent coefficients appearing in Eq. (2). At sufficiently large distances, $r \gg a$, the 2P coupling mobility coincides with the fluid velocity response at a distance $\mathbf{r}$ away from an applied unit force. Using Eq. (2), we get, for the longitudinal part of that mobility, $M_\parallel(r,\omega) = (4\pi\eta_b r)^{-1} + a^2 g(\xi_d/a)(2\pi\eta_\ell r^3)^{-1}$. From the fluctuation-dissipation theorem $D_\parallel(r,\omega) = -(2k_BT/\omega^2)M_\parallel(r,\omega)$, where k_BT is the thermal energy. Comparing this with Eq. (4), we identify

$$A(\tau) = [k_BT/(2\pi)]\mathcal{F}^{-1}\{(-\omega^2\eta_b)^{-1}\}, \tag{5}$$

$$B(\tau) = (k_BT/\pi)a^2 g(\xi_d/a)\mathcal{F}^{-1}\{(-\omega^2\eta_\ell)^{-1}\}, \tag{6}$$

where $\mathcal{F}^{-1}$ denotes the inverse Fourier transform.

Equation (5) merely restates the basic relation used in standard 2P microrheology to measure the bulk viscoelastic moduli. Equation (6) represents our extension. Its left-hand side is a directly measurable coefficient, $B(\tau)$, while its right-hand side depends on two dynamic characteristics of the fluid, η_ℓ and ξ_d. The local response is obtainable from the 1P measurement. According to the GSER, $\mathrm{MSD}^{1P}(\tau) = [k_BT/(3\pi a)]\mathcal{F}^{-1}\{(-\omega^2\eta_\ell)^{-1}\}$ [29]. Substitution in Eq. (6) yields a relation separating the time-dependent observables $\mathrm{MSD}^{1P}(\tau)$ and $B(\tau)$ from the structural features to be characterized, $B(\tau)/\mathrm{MSD}^{1P}(\tau) = 3a^3 g(\xi_d/a)$. Equivalently, we may examine the crossover distance

$$r_c(\tau) = [B(\tau)/A(\tau)]^{1/2} = a[2g(\xi_d/a)]^{1/2}[H(\tau)]^{1/2},$$
$$H(\tau) \equiv \mathrm{MSD}^{1P}(\tau)/\mathrm{MSD}^{2P}(\tau), \tag{7}$$

where the structural part is again decoupled from a measurable time-dependent function, $H(\tau)$, characterizing the ratio between the bulk and local responses. In Fig. 2(a), the experimentally measured r_c is plotted as a function of lag

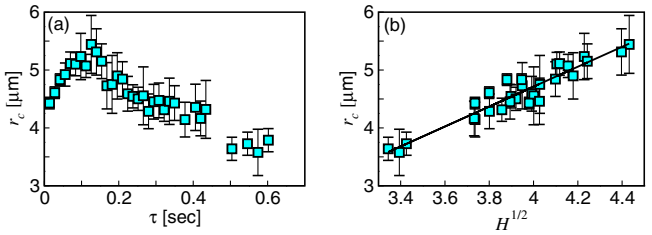

FIG. 2 (color online). Crossover distance as a function of (a) lag time, and (b) square root of $H(\tau)$, the experimental function characterizing the bulk to local viscosity ratio. Parameter values are $a = 0.55$ μm, $\xi_s = 0.44$ μm.

time, exhibiting a nonmonotonic dependence. Yet, by replotting r_c against $[H(\tau)]^{1/2}$, Fig. 2(b), the linear dependence predicted by Eq. (7) is verified. We repeated the analysis for a set of actin networks of different concentrations (i.e., different mesh sizes) and for two different bead sizes. Since the static and dynamic correlation lengths, ξ_s and ξ_d, should be comparable [11], and ξ_s and a are comparable in our experiment, the results should be sensitive to the interpolation function $g(\xi_d/a)$ defined in Eq. (3). In Fig. 3(a), r_c for all the experiments is plotted as a function of $H^{1/2}$. All curves are linear, as predicted, and fall into two clusters (open and filled symbols) corresponding to the two particle sizes. Differentiation of Eq. (3) shows that r_c should increase with either ξ_s or a at constant H, which is confirmed in Fig. 3(a). For a more quantitative validation, we rescale all the measurements according to the scheme suggested by Eq. (7) and obtain convincing data collapse [Fig. 3(b)]. Furthermore, the resulting master curve fits well the theoretical scale function of Eq. (3) using a single free parameter— a constant ratio of order unity between the static and dynamic lengths, $\xi_d = b\xi_s$, with $b \simeq 1.2$–1.3.

One of the new insights in the current Letter is that the local viscoelastic properties of the medium affect its response over length scales much larger than the correlation length and probe size. Moreover, there are scenarios in

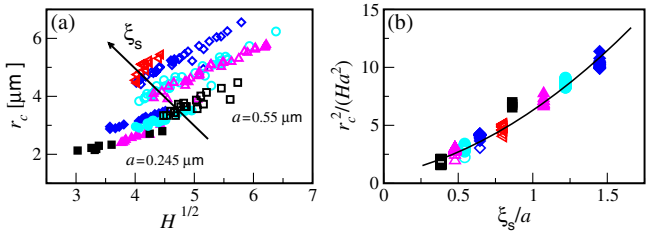

FIG. 3 (color online). Crossover distance for all experiments. (a) For all conditions, r_c is linear with $H^{1/2}$ and increases with either ξ_s or a. (b) All experimental results fall on a master curve once r_c^2 is normalized by Ha^2 and presented as a function of ξ_s/a. The solid line is a fit to Eq. (7) with the scale function given by Eq. (3) and $\xi_d = 1.25\xi_s$. Open (filled) symbols correspond to $a = 0.55(0.245)$ μm. Each color and symbol corresponds to a different mesh size: $\xi_s = 0.21$ (black squares), 0.26 (magenta triangles), 0.3 (cyan circles), 0.35 (blue diamonds), and 0.44 μm (red left triangles).

which the dominant momentum term in the complex-fluid response is suppressed, leaving the subdominant mass term as the sole correlation mechanism at large distances. We mention three examples. (a) For a very stiff matrix, as in the case of a fluid embedded in a solid porous medium, the crossover to the asymptotic term will be pushed to arbitrarily large distances. (b) In a thin film of gel supported on a rigid substrate, the momentum term will be suppressed at distances larger than the film thickness, whereas the mass term will be enhanced by such confinement. This qualitatively accounts for the dipolar shape of the 2P response previously reported for such a system [30]. (c) At sufficiently short time (high frequency), the diffusive momentum term is cut off beyond a certain distance (viscous penetration depth), whereas the mass disturbance, propagating via much faster compression modes, is not. All three scenarios obviously require further quantitative investigation.

Another intrinsic length scale affecting the dynamics of actin networks is the filament length [23]. Its value in the current Letter (13 μm) is much larger than ξ_s and a. For shorter filament lengths, there are subtle effects related to the local environment of the probe [17,23]. Additional length scales, not present in the current system, can arise from sample heterogeneity [31].

Extracting spatiotemporal characteristics such as the dynamic correlation length can be achieved, for example, by various dynamic scattering techniques [2]. The intermediate response itself, however, despite its significant effect demonstrated here, is averaged out in such scattering measurements by virtue of the spatial symmetry of the corresponding dipolar term.

The analysis presented here, clearly, is not restricted to actin networks. It is applicable to any complex fluid with a sufficiently large η_b/η_ℓ contrast [18]. (As "local" refers to the scale of the probe, the contrast can be enhanced by reducing the probe size down to $a \ll \xi_d$, whereupon the local response becomes that of the molecular solvent.) In particular, our findings show that bulk viscoelasticity inadequately describes micron scale stiff biopolymer gels such as the cellular cortical network.

We thank Rony Granek, Fred MacKintosh, and Tom Witten for helpful discussions. This research has been supported by the Israel Science Foundation (Grants No. 1271/08 and No. 8/10) and the Marie Curie Reintegration Grant (No. PIRG04-GA-2008-239378). A. S.-S. acknowledges funding from the Tel-Aviv University Center for Nanoscience and Nanotechnology.

*roichman@tau.ac.il

[1] T. A. Witten, *Structured Fluids* (Oxford University Press, New York, 2004).
[2] R. G. Larson, *The Structure and Rheology of Complex Fluids* (Oxford University Press, New York, 1999).
[3] T. G. Mason and D. A. Weitz, Phys. Rev. Lett. **74**, 1250 (1995).

[4] T. G. Mason, K. Ganesan, J. H. van Zanten, D. Wirtz, and S. C. Kuo, Phys. Rev. Lett. **79**, 3282 (1997).
[5] F. Gittes, B. Schnurr, P. D. Olmsted, F. C. MacKintosh, and C. F. Schmidt, Phys. Rev. Lett. **79**, 3286 (1997); Macromolecules **30**, 7781 (1997).
[6] J. C. Crocker, M. T. Valentine, E. R. Weeks, T. Gisler, P. D. Kaplan, A. G. Yodh, and D. A. Weitz, Phys. Rev. Lett. **85**, 888 (2000).
[7] T. M. Squires and T. G. Mason, Annu. Rev. Fluid Mech. **42**, 413, (2010).
[8] A. J. Levine and T. C. Lubensky, Phys. Rev. Lett. **85**, 1774 (2000); Phys. Rev. E **63**, 041510 (2001).
[9] D. T. Chen, E. R. Weeks, J. C. Crocker, M. F. Islam, R. Verma, J. Gruber, A. J. Levine, T. C. Lubensky, and A. G. Yodh, Phys. Rev. Lett. **90**, 108301 (2003).
[10] L. Starrs and P. Bartlett, Faraday Discuss. **123**, 323 (2003).
[11] P.-G. de Gennes, Macromolecules **9**, 587 (1976); **9**, 594 (1976).
[12] S. T. Milner, Phys. Rev. E **48**, 3674 (1993).
[13] J. Happel and H. Brenner, *Low Reynolds Number Hydrodynamics* (Martinus Nijhoff, The Hague, 1983).
[14] We generalize an argument first presented in H. Diamant, Isr. J. Chem. **47**, 225 (2007).
[15] The local viscosity is a function of ξ_d/a, with $\eta_\ell(\xi_d/a \to \infty) \to \eta$ and $\eta_\ell(\xi_d/a \to 0) \to \eta_b$. Here we bypass this dependence by extracting η_ℓ from 1P measurements.
[16] For simplicity, we neglect inertial effects, which set in at high frequency and can be readily added if needed [8].
[17] Details will be given elsewhere; see also Supplemental Material [26] for a commented Mathematica© file.
[18] V. Pelletier, N. Gal, P. Fournier, and M. L. Kilfoil, Phys. Rev. Lett. **102**, 188303 (2009).
[19] F. C. MacKintosh and A. J. Levine, Phys. Rev. Lett. **100**, 018104 (2008); F. C. MacKintosh and A. J. Levine, J. Phys. Chem. B **113**, 3820 (2009).
[20] Properties (a) and (c) have been qualitatively reported for microtubule networks [18].
[21] A. Palmer, T. G. Mason, J. Y. Xu, S. C. Kuo, and D. Wirtz, Biophys. J. **76**, 1063 (1999).
[22] M. L. Gardel, M. T. Valentine, J. C. Crocker, A. R. Bausch, and D. A. Weitz, Phys. Rev. Lett. **91**, 158302 (2003); J. H. Shin, M. L. Gardel, L. Mahadevan, P. Matsudaira, and D. A. Weitz, Proc. Natl. Acad. Sci. U. S. A. **101**, 9636 (2004).
[23] J. Liu, M. L. Gardel, K. Kroy, E. Frey, B. D. Hoffman, J. C. Crocker, A. R. Bausch, and D. A. Weitz, Phys. Rev. Lett. **96**, 118104 (2006).
[24] M. Atakhorrami, G. H. Koenderink, J. F. Palierne, F. C. MacKintosh, and C. F. Schmidt, arXiv:1210.8404 [Phys. Rev. Lett. (in preparation)].
[25] C. F. Schmidt, M. Barmann, G. Isenberg, and E. Sackmann, Macromolecules **22**, 3638 (1989).
[26] See Supplemental Material at http://link.aps.org/supplemental/10.1103/PhysRevLett.112.088301 for sample preparation details.
[27] J. C. Crocker and D. G. Grier, J. Colloid Interface Sci. **179**, 298 (1996).
[28] J. C. Crocker and B. D. Hoffman, Methods Cell Biol. **83**, 141 (2007).
[29] We use the one-dimensional forms of the MSD's.
[30] G. Ladam, L. Vonna, and E. Sackmann, J. Phys. Chem. B **107**, 8965 (2003).
[31] S. Jabbari-Farouji, M. Atakhorrami, D. Mizuno, E. Eiser, G. H. Wegdam, F. C. MacKintosh, D. Bonn, and C. F. Schmidt, Phys. Rev. E **78**, 061402 (2008).